Theory of thermopower in two-dimensional graphene

E. H. Hwang, E. Rossi, and S. Das Sarma
Condensed Matter Theory Center, Department of Physics, University of Maryland, College Park, Maryland 20742-4111, USA
(Received 16 February 2009; revised manuscript received 4 November 2009; published 9 December 2009)

Motivated by recent experiments by Yuri M. Zuev *et al.* [Phys. Rev. Lett. **102**, 096807 (2009)], Peng Wei *et al.* [Phys. Rev. Lett. **102**, 166808 (2009)], and Joseph G. Checkelsky *et al.* [Phys. Rev. B **80**, 081413(R) (2009)], we calculate the thermopower of graphene incorporating the energy dependence of various transport scattering times. We find that scattering by screened charged impurities gives a reasonable explanation for the measured thermopower. The calculated thermopower behaves as $1/\sqrt{n}$ at high densities, but saturates at low densities. We also find that the thermopower scales with the normalized temperature T/T_F and does not depend on the impurity densities, but strongly depends on the fine-structure constant r_s and on the location of the impurities. We discuss the deviation from the Mott formula in graphene thermopower and use an effective-medium theory to calculate thermopower at low carrier density regimes where electron-hole puddles dominate.

DOI: 10.1103/PhysRevB.80.235415 PACS number(s): 73.50.−h, 81.05.Uw, 72.10.−d, 72.15.Jf

I. INTRODUCTION

Thermopower has been used as a powerful tool to probe transport mechanisms in metals and semiconductors. Often the measurement of resistivity (or conductivity) is inadequate in distinguishing among different scattering mechanisms and the thermopower can then be used as a sensitive probe of transport properties since it provides complementary information to resistivity. In this paper we develop a theory for the thermopower of graphene with a goal toward elucidating the comparative importance of various scattering mechanisms in graphene.[1]

Recently, the thermoelectric properties of graphene have attracted much experimental attention.[2–5] Experimentally[2–4] the expected change of sign in the thermopower is found across the charge neutrality point as the majority carriers change from electrons to holes. Away from the charge neutral region the density dependence of thermopower behaves as $1/\sqrt{n}$, where n is the carrier density, and exhibits a linear temperature dependence in agreement with the semiclassical Mott formula.[6] As the temperature increases, a deviation from Mott formula is reported.[2,3] In this paper we present a calculation of the thermopower of graphene taking into account the energy-dependent scattering time for various scattering mechanisms. Understanding thermopower requires a thorough knowledge of the details of the energy dependence of transport scattering times.[7–9] In metals the Mott formula is widely used because the Fermi temperature is very high (i.e., $T \ll T_F$), and the scattering time is essentially energy independent leading to a simple linear-in-temperature form for thermopower that is proportional to the energy derivative of the conductivity evaluated at the Fermi energy. The Mott formula, derived mathematically through the Sommerfeld expansion, is only valid at very low temperatures, $T/T_F \ll 1$. Previous theoretical works[10] on graphene thermopower did not consider different possible scattering mechanisms, did not focus on the scattering due to charged impurities, and so did not consider the additional temperature dependence due to screening. Moreover, they all considered only the low-temperature limit using the Mott formula to calculate the thermopower and so their results are not applicable in the high-temperature range, in which deviations from the Mott formula are observed.[2–4]

We show that scattering by random charged impurity centers, which is the main scattering mechanism limiting graphene conductivity,[11] also dominates its thermopower. We find the effects of short-range scattering and phonons to be negligible in experimental temperature range ($T < 300$ K). Substrate acoustic phonons and/or graphene acoustic phonons can induce a phonon-drag component Q_d for the thermopower. In general Q_d depends on the temperature with a power much higher than 1 (Refs. 8 and 9): $Q_d \propto T^4$. However, the measured thermopower[2–4] even at the highest temperatures strongly indicates the absence of a phonon-drag component. This is due to the weak electron-phonon (e-h) coupling in graphene; we therefore ignore the phonon-drag contribution. We show that the temperature-dependent screening effects[12] must be included in the theory to get quantitative agreement with existing experimental data. We also find that the calculated thermopower scales with T/T_F and manifests no impurity density (n_i) dependence, but depends strongly on the impurity location and on the dielectric constant of the substrate (or equivalently the fine-structure constant of graphene). The experimentally observed asymmetry between electron and hole thermopower is explained by the asymmetry in the charged impurity configuration in the presence of the gate voltage. We explain the experimentally observed sign change near the charge neutrality point (Dirac point) with a simple two-component model, which we explicitly verify using an effective-medium theory (EMT) that takes into account the presence of electron-hole puddles.[11]

The paper is organized as follows. In Sec. II the general theory of graphene thermopower is presented by considering the energy dependence of various transport scattering rates. Section III presents the results of the calculations. We conclude in Sec. IV with a discussion.

II. THEORY

The ratio of the measured voltage to the temperature gradient applied across the sample is known as the Seebeck coefficient (or the thermopower) and is given by $Q = \nabla V/\nabla T$, where ∇V is the potential difference and ∇T is the temperature difference between two points of the sample.[7] In

linear-response approximation for the electrical current density $\mathbf{j}$ and thermal current density $\mathbf{j}_Q$, we have

$$\mathbf{j} = L^{11}\mathbf{E} + L^{12}(-\nabla T), \tag{1a}$$

$$\mathbf{j}_Q = L^{21}\mathbf{E} + L^{22}(-\nabla T), \tag{1b}$$

where L^{ij} is defined in terms of the integrals $I^{(\alpha)}$: $L^{11}=I^{(0)}$, $L^{12}=-\frac{1}{eT}I^{(1)}$, $L^{21}=-\frac{1}{e}I^{(1)}$, and $L^{22}=(1/e^2T)I^{(2)}$, where

$$I^{(\alpha)} = e^2 g \sum_{\mathbf{k}} \tau(\epsilon_{\mathbf{k}}) \mathbf{v}_{\mathbf{k}} \mathbf{v}_{\mathbf{k}} [\epsilon_{\mathbf{k}} - \mu]^{\alpha} \left(-\frac{\partial f^0_{\mathbf{k}}}{\partial \epsilon_{\mathbf{k}}} \right)$$

$$= \int d\varepsilon (\varepsilon - \mu)^{\alpha} \left(-\frac{\partial f^0(\varepsilon)}{\partial \varepsilon} \right) \sigma(\varepsilon). \tag{2}$$

Here, $\epsilon_{\mathbf{k}}=v_F|\mathbf{k}|$, $f^0_{\mathbf{k}}$ is the equilibrium Fermi distribution function, τ is the relaxation time, μ is the chemical potential, $g=g_s g_v$ is the total degeneracy (with $g_s=2$ and $g_v=2$ being the spin and valley degeneracies, respectively), and $\sigma(\varepsilon)$ is the energy-dependent conductivity of graphene given by

$$\sigma(\varepsilon) = e^2 v_F^2 D(\varepsilon) \tau(\varepsilon)/2, \tag{3}$$

where v_F is the Fermi velocity and $D(\varepsilon)=g|\varepsilon|/(2\pi\hbar^2 v_F^2)$ is the density of states. Notice that $L^{11}=\sigma(\varepsilon=0)$. From the definition of the thermopower we have $Q=L^{12}/L^{11}$.

Before we calculate the details of the thermopower for different scattering mechanisms we first consider the low- and high-temperature behaviors of $Q(T)$. At low temperatures ($T \ll T_F$, where $T_F=E_F/k_B$) we can express $I^{(\alpha)}$ as

$$I^{(\alpha)} = \frac{1}{4\beta^{\alpha}} \int_{-\infty}^{\infty} dx \frac{x^{\alpha}}{\tanh^2(x/2)} \left[\sigma(\mu) + \frac{x}{\beta} \left. \frac{\partial \sigma(\varepsilon)}{\partial \varepsilon} \right|_{\varepsilon=\mu} \right], \tag{4}$$

where $\beta=1/k_BT$. Thus, we have the well-known Mott formula[6] of thermopower, i.e.,

$$Q = -\frac{\pi^2}{3e} \frac{T}{\sigma(\mu)} \left. \frac{\partial \sigma(\varepsilon)}{\partial \varepsilon} \right|_{\varepsilon=\mu}. \tag{5}$$

If the energy dependence of the relaxation time is unimportant the sign of the thermopower is determined by whether the carriers are electrons or holes. Assuming the energy-dependent scattering time to be $\tau \propto \varepsilon^m$ we have the thermopower at low temperatures,

$$Q = -\frac{\pi^2}{3e} \frac{k_B T}{T_F} (m+1). \tag{6}$$

As explained below different values of m correspond to different scattering mechanisms. In general "m" has weak temperature and density dependence since τ behaves only as an effective power law in energy. Equation (6) indicates that the thermopower can change sign if $m<-1$. At high temperatures ($T \gg T_F$) we can express $I^{(\alpha)}$ with an energy-dependent scattering time $\tau=\tau_0 \varepsilon^m$ as

$$I^{(\alpha)} \approx E_F^{\alpha} \left(\frac{T}{T_F} \right)^{\alpha+m+1} \left[1 - \frac{1}{2^{\alpha+m}} \right] \Gamma(\alpha+m+2) \zeta(\alpha+m+1), \tag{7}$$

where $\Gamma(z)$ and $\zeta(z)$ are the gamma and Riemann's zeta functions, respectively, from which we find

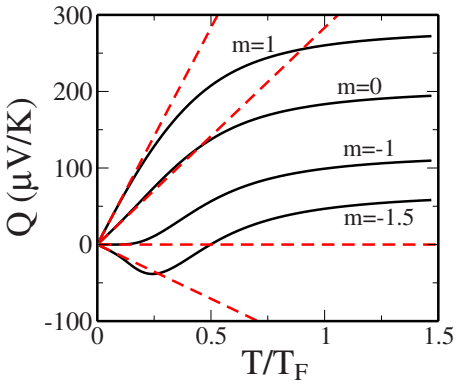

FIG. 1. (Color online) Hole thermopower for different energy-dependent scattering times, $\tau \propto \varepsilon^m$. For $m<-1$ the low-temperature thermopower becomes negative. Dashed lines show the Mott formula for the corresponding scattering times. Electron results are the same with an overall negative sign.

$$Q \approx -\frac{k_B}{e} \frac{(m+2)}{2} \frac{(2^{m+1}-1)}{(2^m-1)} \frac{\zeta(m+2)}{\zeta(m+1)}. \tag{8}$$

At high temperatures graphene thermopower is independent on temperature and approaches a limiting value. In Fig. 1 we show the calculated graphene thermopower for different exponents m ($\tau \propto \varepsilon^m$) as a function of T/T_F. As shown in Fig. 1 the dashed lines representing the Mott formula agree with the full calculations for $T \lesssim 0.2T_F$. In addition the calculated thermopower scales as a function of the normalized temperature (T/T_F).

Now we calculate the thermopower in the presence of various physical scattering mechanisms. For both neutral white-noise short-range disorder and acoustic phonon[13] scattering, we can express the scattering time as $\tau(\epsilon)=\tau_1/\epsilon$, i.e., $m=-1$. Thus, the Mott formula of Eq. (6) indicates that $Q=0$, but from the direct calculation of Eq. (2) we have

$$I^{(0)} = \sigma_1 \frac{1}{1+e^{-\beta\mu}}, \tag{9a}$$

$$I^{(1)} = \sigma_1 \left[k_B T \ln[1+e^{-\beta\mu}] + \frac{\mu}{1+e^{\beta\mu}} \right]. \tag{9b}$$

Then the thermopower becomes

$$Q = -\frac{1}{e} \left[\frac{\mu}{T} e^{-\beta\mu} + O(e^{-\beta\mu}) \right]. \tag{10}$$

The thermopower contributions from both neutral scatterers and acoustic phonons are exponentially suppressed in the low-temperature limit and can be ignored. For unscreened charged impurities we have an energy-dependent scattering time[12] $\tau(\epsilon)=\tau_0\epsilon$. Then we have the following integrals for $t=T/T_F \ll 1$:

$$I^{(0)} = \sigma_0[1 + O(e^{-\beta\mu})], \tag{11a}$$

$$I^{(1)} = \sigma_0 E_F\left[\frac{2\pi^2}{3}t^2 + O(e^{-\beta\mu})\right], \tag{11b}$$

leading to the thermopower

$$Q = -\frac{2\pi^2}{3e}\frac{k_B^2 T}{E_F}[1 + O(e^{-\beta\mu})]. \tag{12}$$

The linear dependence of thermopower on temperature (or the Mott formula) holds to relatively high temperatures in graphene for unscreened Coulomb impurities.

As it has been demonstrated theoretically[11,14] and experimentally[15] the dominant transport mechanism in graphene is the screened Coulomb scattering from charged impurities. The result of Eq. (12) for unscreened Coulomb scattering is much higher than the thermopower observed in experiments[2–4] and cannot explain the behavior of Q close to the Dirac point. An accurate quantitative agreement between theory and experiment can only be achieved by taking into account the screening of the charged impurities and the strong spatial inhomogeneity that these impurities induce close to the Dirac point. For the screened charged impurity scattering, the energy-dependent scattering time $\tau(\varepsilon_k)$ is given by[11]

$$\frac{1}{\tau(\epsilon_k)} = \frac{\pi n_i}{\hbar}\int \frac{d^2k'}{(2\pi)^2}\left|\frac{v_i(q)}{\epsilon(q,T)}\right|^2 \delta(\epsilon_{\mathbf{k}} - \epsilon_{\mathbf{k}'})(1 - \cos\theta)(1 + \cos\theta), \tag{13}$$

where θ is the scattering angle, $v_i(q) = 2\pi e^2 \exp(-qd)/(\kappa q)$ is the Fourier transform of the two-dimensional (2D) Coulomb potential in an effective background lattice dielectric constant κ, and d is the average distance of the charged impurities from the graphene layer. In Eq. (13), $\varepsilon(q) \equiv \varepsilon(q,T)$ is the 2D finite-temperature static random phase approximation (RPA) dielectric (screening) function appropriate for graphene,[12] given by $\varepsilon(q,T) = 1 + v_c(q)\Pi(q,T)$, where $\Pi(q,T)$ is the graphene irreducible finite-temperature polarizability function and $v_c(q)$ is the Coulomb interaction. There is an important direct T dependence of thermopower, not captured in the Mott formula, arising from the temperature-dependent screening.[12] The temperature-dependent conductivity due to screening effects decreases quadratically at low temperatures.[12] This mechanism produces a thermopower quadratic in temperature rather than linear as in the simple Mott formula. Thus, we predict a nonlinear quadratic temperature correction in the graphene thermopower compared with the linear Mott formula.

III. RESULTS

In Fig. 2(a) we show the calculated thermopower of holes in graphene due to different scattering mechanisms. Note that electron results are the same with an overall negative sign. The thermopower due to screened charged impurity is about half of that due to the unscreened charged impurities and increases in a concave manner due to temperature- and energy-dependent screening. On the other hand, the thermopower due to neutral scatterers is exponentially suppressed in the low-temperature regime. Figure 2(b) shows the calculated thermopower for the screened charged impurity scattering as a function of density for different temperatures. As we expect the density dependence shows $1/\sqrt{n}$ behavior at high densities. This power law behavior breaks down and saturates at low densities. The saturation value (Q_s) does not depend on temperature. The theoretical Q_s is just a function of interaction (fine-structure) parameter $r_s = e^2/\kappa\hbar v_F$ and the location of impurities d. In Figs. 2(c) and 2(d) we show $Q(T)$ for the case of screened charged impurities for different values of r_s and d, where d is the location of the charged impurity measured from the graphene sheet. In general the thermopower increases when the substrate dielectric constant (κ) increases or the charged impurities move away. Thus, we predict that the thermopower of suspended graphene will decrease compared with the thermopower of graphene on a substrate for the same impurity density be-

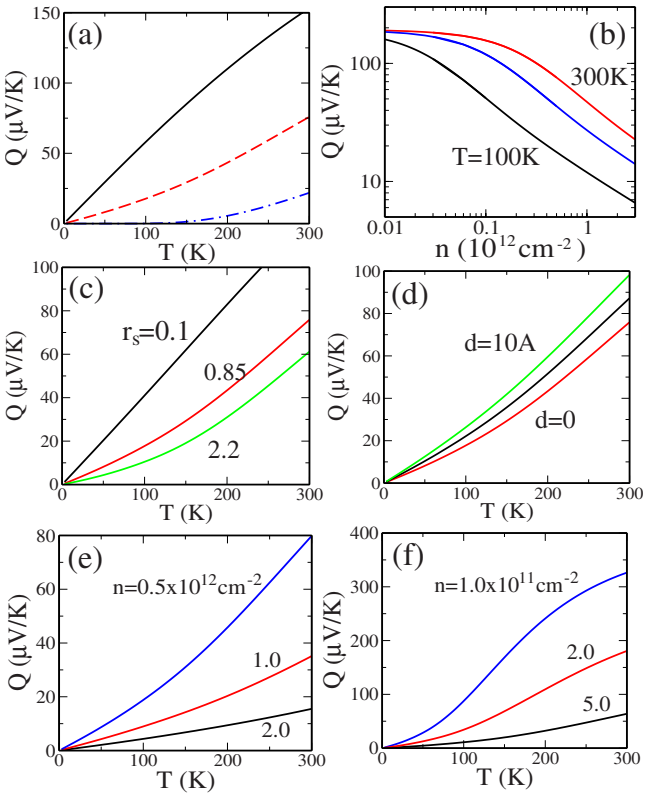

FIG. 2. (Color online) (a) Q as a function of temperature for different scattering mechanisms. Solid, dashed, and dotted-dashed lines represent unscreened Coulomb, screened Coulomb, and neutral scatterers, respectively. (b) Q for the screened charged impurity scattering as a function of density for different temperatures. (c) Q for different $r_s = 0.1, 0.85, 2.2$ with $d = 0$ and (d) for different $d = 0, 5, 10$ Å with $r_s = 0.85$. Here, d is the location of the charged impurity measured from the graphene sheet. In (a)–(d) we use $n = 5 \times 10^{11}$ cm^{-2}. In (e) and (f), Q in the presence of screened charged impurities for different densities is shown. In (e) we use parameters corresponding to graphene on SiO_2 with mobility $\mu = 10^4$ cm^2/V s, and in (f) to suspended graphene with mobility $\mu = 2 \times 10^5$ cm^2/V s.

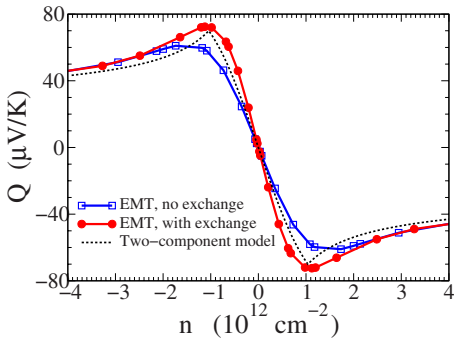

FIG. 3. (Color online) Q due to the screened charge impurities as a function of density close to the Dirac point for $T=300$ K, $n_i=10^{12}$ cm^{-2}, $r_s=0.8$, and $d=1$ nm, obtained using the two-component model and the EMT with and without exchange energy.

cause of the reduction in the dielectric constant. In Figs. 2(e) and 2(f) we show the calculated thermopower for systems with different mobilities due to screened charged impurity scattering for graphene on SiO_2 substrate and for suspended graphene.

In recent experiments[2–4] it has been observed that close to the Dirac point Q does not follow the $1/\sqrt{n}$ scaling predicted by the Mott formula. The reason for this deviation is that close to the Dirac point the quenched disorder induces strong density fluctuations that break up the density landscape in electron-hole puddles.[11,16–19] To account for the main features of the thermopower close to the Dirac point, we can use a simple two-component model in which the electron density n_e and the hole density n_h depend on the doping n according to the phenomenological equations: $n_e=(n_{\rm rms}+n)/2$ and $n_h=(n_{\rm rms}-n)/2$ for $|n|\le n_{\rm rms}$, where $n_{\rm rms}$ is the root mean square of the density fluctuations. For exfoliated graphene we have $n_{\rm rms}\sim n_i$.[11,17] In the two-component model the thermopower becomes

$$Q=(L_e^{12}+L_h^{12})/(L_e^{11}+L_h^{11}), \tag{14}$$

so that, for unscreened charged impurities, we find

$$Q=-\frac{k_B^2}{e}\frac{2\pi^2}{3}\frac{T}{v_F\sqrt{\pi}}\left[\frac{\sqrt{|n_e|}-\sqrt{|n_h|}}{|n_e|+|n_h|}\right]. \tag{15}$$

Thus, if there is an equal number of electrons and holes the thermopower goes to zero, and the overall sign is decided by the majority carriers. Using the two-component model for the screened charge impurities case for $Q(n)$, we find the results shown by the dashed line in Fig. 3.

In the presence of charge impurities the density profile close to the Dirac point, where the total carrier density $n<n_{\rm rms}\sim n_i$,[17] is quantitatively described by the Thomas-Fermi-Dirac (TFD) theory.[19] Using the TFD results the transport properties of graphene close to the Dirac point can be accurately calculated using the EMT. The EMT approach is valid when the mean free path is much smaller than the size L_p of the typical e-h puddle and the resistance across the puddle boundaries is smaller than the resistance inside the puddles. It turns out that these two conditions are equivalent and satisfied whenever $L_p\gg 1/\sqrt{n_i}$.[19] For current experiments this inequality is always satisfied because L_p is on the order of the sample size[19] and $n_i>10^{10}$ cm^{-2}. The fact that the resistance due to the puddle boundaries can be neglected relies on (a) the Klein paradox[20] and (b) the fact that for large values of L_p the length of the puddle boundary is very large. Denoting by angular brackets the disordered averaged quantities, for the diagonal transport coefficients in two dimensions, the *effective-medium* coefficients $L_{\rm eff}^{ii}$ are implicitly given by the equation[21]

$$\left\langle\frac{L^{ii}(\mathbf{r})-L_{\rm eff}^{ii}}{L^{ii}(\mathbf{r})+L_{\rm eff}^{ii}}\right\rangle=0. \tag{16}$$

Adapting to two dimensions the results presented in Ref. 22, the effective-medium off-diagonal coefficient L^{12} is given by

$$L_{\rm eff}^{12}=-2L_{\rm eff}^{11}L_{\rm eff}^{22}\left\langle\frac{L^{12}(\mathbf{r})}{[L^{11}(\mathbf{r})+L_{\rm eff}^{11}][L^{22}(\mathbf{r})+L_{\rm eff}^{22}]}\right\rangle \times\left\langle\frac{L^{11}(\mathbf{r})L_{\rm eff}^{22}+L_{\rm eff}^{11}L^{22}(\mathbf{r})+L_{\rm eff}^{11}L_{\rm eff}^{22}-L^{11}(\mathbf{r})L^{22}(\mathbf{r})}{[L^{11}(\mathbf{r})+L_{\rm eff}^{11}][L^{22}(\mathbf{r})+L_{\rm eff}^{22}]}\right\rangle^{-1}, \tag{17}$$

where $L^{ij}(\mathbf{r})=L^{ij}(n(\mathbf{r}))$. Using Eqs. (16) and (17) and the probability distribution given by the TFD theory, we can calculate the effective-medium thermopower $Q_{\rm eff}=L_{\rm eff}^{12}/L_{\rm eff}^{11}$ at (and away from) the Dirac point. The results for $Q_{\rm eff}$ as a function of n at $T=300$ K for $r_s=0.8$, $d=1$ nm, and $n_i=10^{12}$ cm^{-2} are shown by the solid lines in Fig. 3; in squares (circles) are the results obtained with (without) the effect of the exchange term on the density distribution. We note that the two-component model is excellent in describing the main features of the realistic EMT $Q(n)$ close to the Dirac point.

IV. CONCLUSION

In conclusion we have developed a complete theory for the diffusive thermopower of 2D graphene. Quantitative agreement between our theory and existing graphene experimental thermopower data is a strong indication that the dominant carrier scattering mechanism operational in 2D graphene monolayers is the screened Coulomb scattering by random charged impurities located in the graphene environment. Other defects[23] (resonant scatterers and midgap states) which also give the linear density-dependent conductivity predict a logarithmic correction in density-dependent thermopower. However, there is no direct observation of this correction in the measured thermopower.[2–4] At high densities the Mott formula applies well to the measured thermopower because of the high Fermi temperature, but it fails in the low-density limit. We explain the sign change of the thermopower in the low-density regime by using both a two-component model and a realistic effective-medium theory, which correctly describes transport in the presence of the strong carrier density inhomogeneities that characterize the graphene density landscape close to the Dirac point. We make a number of specific predictions for graphene thermopower (e.g., nonlinearity in temperature, existence of a saturation thermopower at low densities, and nontrivial dependence on the background dielectric constant and on the

impurity location), which should be tested experimentally in order to conclusively settle the issue of dominant carrier scattering mechanism in graphene.

We would also like to note that we recently become aware of the related works.[24,25]

ACKNOWLEDGMENTS

This work was supported by the US-ONR and NSF-NRI-SWAN. E.H.H. acknowledges the hospitality of the KITP at UCSB while this work was partially fulfilled.

[1] A. H. Castro Neto, F. Guinea, N. M. R. Peres, K. S. Novoselov, and A. K. Geim, Rev. Mod. Phys. **81**, 109 (2009).
[2] Yuri M. Zuev, W. Chang, and P. Kim, Phys. Rev. Lett. **102**, 096807 (2009).
[3] Peng Wei, W. Bao, Y. Pu, C. N. Lau, and J. Shi, Phys. Rev. Lett. **102**, 166808 (2009).
[4] Joseph G. Checkelsky and N. P. Ong, Phys. Rev. B **80**, 081413(R) (2009).
[5] A. A. Balandin, S. Ghosh, W. Bao, I. Calizo, D. Teweldebrhan, F. Miao, and C. N. Lau, Nano Lett. **8**, 902 (2008).
[6] M. Cutler and N. F. Mott, Phys. Rev. **181**, 1336 (1969).
[7] N. W. Ashcroft and N. D. Mermin, *Solid State Physics* (Thomson Learning Inc., New York, 1976).
[8] L. Moldovan, S. Melinte, V. Bayot, S. J. Papadakis, E. P. De Poortere, and M. Shayegan, Phys. Rev. Lett. **85**, 4369 (2000).
[9] S. K. Lyo, Phys. Rev. B **70**, 153301 (2004).
[10] T. Löfwander and M. Fogelström, Phys. Rev. B **76**, 193401 (2007); T. Stauber, N. M. R. Peres, and F. Guinea, *ibid.* **76**, 205423 (2007); B. Dóra and P. Thalmeier, *ibid.* **76**, 035402 (2007); M. S. Foster and I. L. Aleiner, *ibid.* **77**, 195413 (2008); M. Müller, L. Fritz, and S. Sachdev, *ibid.* **78**, 115406 (2008).
[11] E. H. Hwang, S. Adam, and S. Das Sarma, Phys. Rev. Lett. **98**, 186806 (2007); S. Adam, E. H. Hwang, V. M. Galitski, and S. Das Sarma, Proc. Natl. Acad. Sci. U.S.A. **104**, 18392 (2007).
[12] E. H. Hwang and S. Das Sarma, Phys. Rev. B **79**, 165404 (2009); **75**, 205418 (2007).
[13] E. H. Hwang and S. Das Sarma, Phys. Rev. B **77**, 115449 (2008).
[14] K. Nomura and A. H. MacDonald, Phys. Rev. Lett. **96**, 256602 (2006); T. Ando, J. Phys. Soc. Jpn. **75**, 074716 (2006); V. V. Cheianov and V. I. Fal'ko, Phys. Rev. Lett. **97**, 226801 (2006).
[15] Y. W. Tan, Y. Zhang, K. Bolotin, Y. Zhao, S. Adam, E. H. Hwang, S. Das Sarma, H. L. Stormer, and P. Kim, Phys. Rev. Lett. **99**, 246803 (2007); J. H. Chen, C. Jang, S. Adam, M. S. Fuhrer, E. D. Williams, and M. Ishigami, Nat. Phys. **4**, 377 (2008).
[16] J. Martin, N. Akerman, G. Ulbricht, T. Lohmann, J. H. Smet, K. von Klitzing, and A. Yacoby, Nat. Phys. **4**, 144 (2008); Y. Zhang, V. W. Brar, C. Girit, A. Zettl, and M. F. Crommie, *ibid.* **5**, 722 (2009).
[17] E. Rossi and S. Das Sarma, Phys. Rev. Lett. **101**, 166803 (2008).
[18] M. Polini, A. Tomadin, R. Asgari, and A. H. MacDonald, Phys. Rev. B **78**, 115426 (2008).
[19] E. Rossi, S. Adam, and S. Das Sarma, Phys. Rev. B **79**, 245423 (2009); M. Fogler, arXiv:0810.1755 (unpublished).
[20] V. V. Cheianov and V. I. Fal'ko, Phys. Rev. B. **74**, 041403(R) (2006).
[21] D. A. G. Bruggeman, Ann. Phys. (N.Y) **416**, 636 (1935); R. Landauer, J. Appl. Phys. **23**, 779 (1952).
[22] I. Webman, J. Jortner, and M. H. Cohen, Phys. Rev. B **16**, 2959 (1977).
[23] D. M. Basko, Phys. Rev. B **78**, 115432 (2008); M. I. Katsnelson and A. K. Geim, Philos. Trans. R. Soc. London, Ser. A **366**, 195 (2008).
[24] Y. Ouyang and J. Guo, Appl. Phys. Lett. **94**, 263107 (2009).
[25] X. Z. Yan, Y. Romiah, and C. S. Ting, Phys. Rev. B **80**, 165423 (2009).